International Journal of Thermofluid Science and Technology (2024)
Volume 11, Issue 1, Paper No. 110103
https://doi.org/10.36963/IJTST.2024110103

Research Article

Enhancing Electronics Cooling with Al2O3-Ag/Ethylene Glycol Hybrid Nanofluids

Sid Ali Si Salah*

Faculty of Mechanical and Process Engineering, Houari Boumedienne University, B.P. 32 El Alia, Algiers, Algeria,

ATICLE INFO

Received: 19 Nov. 2023;
Received in revised form:
10 Dec. 2023;
Accepted: 15 Dec. 2023;
Published online:
20 Dec. 2023

Keywords:
Numerical modelling, Hybrid Nanofluids, microchannel heat sink, Heat transfer enhancement.

ABSTRACT

This study utilized a homogeneous phase model to examine the laminar forced convection flow within a broad rectangular micro-channel. It involved the use of nanofluids composed of alumina (Al_2O_3) and a combined mixture of Al_2O_3 and silver (Ag) particles suspended in ethylene glycol as the base fluid. A finite thickness was attributed to the bottom of the micro-channel to provide space for a heat source or electronic component. The study explored various parameters, including nanoparticle diameter, concentration, hybrid nanoparticle mixture volume fractions, and Reynolds number, to analyze the flow and heat transfer characteristics within the micro-channel. To validate the computational method, experimental data from the literature for Al_2O_3/water nanofluids were successfully used as a reference. The findings of this investigation revealed that a nanofluid consisting of 4% hybrid nanoparticles (0.8% Al_2O_3 + 3.2% Ag) exhibited a higher average convective heat transfer coefficient compared to pure ethylene glycol and pure alumina (Al_2O_3). This suggests that hybrid nanofluids represent a promising new class of working fluids for enhancing heat transfer. Furthermore, the study found that the average convective heat transfer coefficient is enhanced by 83% compared to pure ethylene glycol (EG) with higher Reynolds numbers and volume concentrations of nanoparticles. Additionally, there was a 58% increase in the convective heat transfer coefficient with smaller nanoparticle diameters. Importantly, the use of hybrid nanofluids with different volume fractions and nanoparticle diameters did not significantly affect the friction factor within the micro-channel.

1. Introduction

The study of flow and heat transfer properties in microsystems has gained substantial attention due to advances in microelectromechanical systems (MEMS) and micrototal analysis systems. These innovations have far-reaching implications across fields like microelectronic cooling, microheat exchangers, bioengineering, the human genome project, and

*Corresponding e-mail: ssi-salah@usthb.dz (Sid Ali Si Salah)

Nomenclature

Cp	Specific heat, J/kg K		
D_h	hydraulic diameter, m	x	axial coordinate, m
d_{np}	nanoparticle diameter, nm	y	Transversal coordinate, m
h_f	microchannel inlet height, m		
h_s	microchannel thickness, m	*Greek symbols*	
h	heat transfer coefficient, W/m^{2}K	ρ	density, kg/m^3
k	Thermal conductivity, W/m K	μ	dynamic viscosity, *kg/m. s*
L	Microchannel length, m	ϕ	Volume concentration
$f.Re$	Poiseuille number	α	Thermal diffusivity, m^2/s
p	pressure, Pa		
q_0	Heat flux, W/m^2	*Subscripts*	
Re	Reynolds number	b_f	base fluid
u	Axial component of velocity, m/s	n_f	nanofluid
v	transversal component of velocity, m/s	np	nanoparticle
u_{in}	inlet velocity, m/s		

medical engineering. Understanding microscale phenomena is crucial for designing effective microdevices. Microchannel heat sinks offer a major advantage with significantly higher heat transfer coefficients compared to traditional heat exchangers, making them attractive for future micro- and nanotechnologies. Initially, water was the primary coolant, but its limitations led to the search for alternatives, such as solid particles like silver, which have superior thermal conductivity. In 1995, Choi [1] introduced nanofluids, dispersing nanosized particles in base fluids like water or ethylene glycol as coolants for liquid cooling systems. Extensive research, both on micro and macro scales, has enhanced our knowledge of nanofluid behavior, highlighting their potential to improve heat transfer efficiency at both levels.

Lee and Mudawar [2] utilized Al_2O_3 nanofluid mixed with water in a microchannel with a low concentration. They observed increased heat transfer coefficients specifically in the entrance region of the microchannel. However, they concluded that nanofluids might not be suitable for use in two-phase microchannels. Chein and Chung [3] investigated the impact of Al_2O_3-H_2O nanofluid on the heat transfer performance of a trapezoidal microchannel. They found that at low flow rates, nanofluid outperformed pure water in terms of heat transfer. Bianco et al. [4] conducted a numerical study on forced convection of nanofluid in a round tube. Their results showed significant heat transfer enhancement with ncreasing nanofluid volume percentage. The highest heat transfer coefficient and Nusselt number were achieved when the temperature difference between the wall and bulk fluid was minimized. This improved heat transfer performance may be attributed to reduced shear stress due to temperature rise.

In their experiments, Ho et al. [5] explored forced convective heat transfer using Al_2O_3-H2O nanofluid in a rectangular microchannel. They found that the heat sink employing nanofluid as a coolant exhibited higher average heat transfer coefficients, lower thermal resistance, and lower wall temperatures, particularly under high pumping power, compared to pure water.

Sajadi and Kazemi [6] noted that at a Reynolds number of 5000, the use of TiO_2/water nanofluid at volume concentrations of 0.05% and 0.25% resulted in heat transfer improvements of 19% and 22%, respectively. Suresh et al. [7] conducted experiments to investigate the impact of Al_2O_3-Ag/water hybrid nanofluid on laminar heat transfer characteristics in a uniformly heated circular tube. They observed a 13.56% increase in the Nusselt number compared to using water, at a

Reynolds number of 1730. Mohammad Kalteh et al. [8] conducted a study examining the laminar convective heat transfer of an alumina-water nanofluid flowing within a wide rectangular microchannel heat sink (with dimensions of 94.3 mm in length, 28.1 mm in width, and 580 μm in height) both through numerical simulations and experimental observations. For the experimental part of the study, a microchannel was fabricated using a silicon wafer with glass layers. In the numerical analysis, a two-phase Eulerian-Eulerian method employing the finite volume approach was employed. A comparison of the experimental and numerical findings revealed that the two-phase approach yielded results that closely matched the experimental data, surpassing the accuracy of the homogeneous (single-phase) modeling. The maximum deviation from the experimental results was 12.61% for the homogeneous method and 7.42% for the two-phase method, indicating that the two-phase method was more suitable for simulating nanofluid heat transfer. Furthermore, the two-phase results indicated that the velocity and temperature differences between the phases were minimal and negligible. Additionally, the average Nusselt number increased with higher Reynolds numbers and volume concentrations, while it decreased with smaller nanoparticle sizes.

Xin Fang et al. [9] conducted a study on ethylene glycol-based suspensions containing silver nanoparticles of different shapes. They observed that with a volume concentration of 0.1%, silver nanowires led to an enhancement in thermal conductivity of up to 15.6%. Shariat et al. [10] investigated the influence of nanoparticle mean diameter and buoyancy force on laminar mixed convection nanofluid flow within an elliptic duct, employing a two-phase mixture model. Their findings indicated that, under specific Reynolds and Richardson number conditions, a decrease in nanoparticle diameter and an increase in the Richardson number resulted in an increase in the average Nusselt number.

Farhad Abbassi et al. [11] conducted research on the flow behavior of CuO nanofluid within a microchannel. They found that as the expansion ratio of the microchannel decreased, there was an enhancement in the average Nusselt number. Omid Ali Akbari et al. [12] carried out a numerical exploration to investigate the heat transfer characteristics of Water/CMC-Alumina nanofluids with solid nanoparticle volume fractions of 0.5% and 1.5% in a rectangular microchannel with a length (L) of 2500μm and a hydraulic diameter (Dh) of 25μm. Their findings indicated that increasing the volume fraction of solid nanoparticles and reducing the nanoparticle diameter led to an enhancement in heat transfer, particularly at higher Reynolds numbers.

Vivek Kumar and Jahar Sarkar [13] conducted a recent study on nanofluid-cooled mini-micro channel heat sinks, known for their compactness and improved heat transfer capabilities. They performed numerical simulations comparing DI water-based Al_2O_3 nanofluid and Al_2O_3-MWCNT hybrid nanofluid in a minichannel heat sink, employing a two-phase mixture model to analyze heat transfer and pressure drop. Experimental validation was also carried out. The study examined parameters such as hydraulic diameter, channel aspect ratio, composition of Al_2O_3 and MWCNT in the hybrid nanofluid, and Reynolds number. The two-phase model demonstrated better agreement with experimental data. The highest heat transfer coefficient was found for the 0.01 vol% (Al2O3 + MWCNT) (7:3) hybrid nanofluid with a minichannel depth of 0.5 mm. Using nanofluids increased the developing length, and employing hybrid nanofluids resulted in a 15.6% improvement in maximum heat transfer coefficient without a significant rise in pressure drop.

M. K. Nayak [14] performed a study to analyze the effects of homogeneous and heterogeneous reactions, a variable magnetic field, and thermal radiation on the three-dimensional flow of an incompressible nanofluid over an exponentially stretching sheet subject to convective boundary conditions. This study aimed to enhance heat transfer using the Patel model. The governing differential equations were transformed and solved using the fourth-order Runge-Kutta method in conjunction with a shooting technique, while the secant method was employed for improved

approximation. The key finding of this computational study was that the magnetic field interaction hindered fluid motion, resulting in reduced wall shear stresses (both axial and transverse), and the homogeneous and heterogeneous parameters had a significant impact on fluid concentration.

S S Ghadikolaei and M Gholinia [15] investigated natural convection Magnetohydrodynamics MHD flow of Cu/ethylene glycol-water nanofluid past a porous vertical sheet. They used RKF 5 (Runge- Kutta Fehlberg fifth order) method to analyze effects of radiation, shape, slip, and suction/injection. Results show thermal radiation enhances temperature, especially with lamina-shaped nanoparticles, which also boosts Nusselt number more than hexahedron.

M Veera Krishna and Ali J Chamkha [16] investigated magnetohydrodynamic squeezing flow of a water-based nanofluid through a porous medium between two parallel disks, considering Hall current. They employed the Galerkin optimal homotopy asymptotic method for solutions. The study examined effects of various parameters on velocity, temperature, and concentration through graphs, and provided numerical results for local Nusselt and Sherwood numbers. Suction/blowing, squeeze, Hartman number, Hall parameter, Brownian motion, and thermophoresis were analysed Suction flow had a significant impact on concentration field compared to blowing. Brownian motion and thermophoresis increased temperature and nanoparticle concentration. The results were in good agreement with existing literature under similar assumptions.

In another study, M Veera Krishna and Ali J Chamkha [17] studied the influence of Hall and ion slip effects on magnetohydrodynamic free convective rotating flow of nanofluids past a vertical semi-infinite flat plate in a porous medium. Using perturbation approximation, they analytically solved the governing flow equations. The study revealed that velocity increased with Hall and ion slip parameters, while convective parameter amplified thermal boundary layer thickness. Heat generation parameter had an opposite effect. Skin friction coefficient varied with nanoparticle volume fraction, Hall, and ion slip parameters. The study suggested potential applications in cancer cell destruction during drug delivery.

Vivek Kumar and Jahar Sarkar [18] conducted an experimental analysis of minichannel heat sink using hybrid nanofluids comprising various nanoparticles mixed with deionized water. They considered combinations of Al2O3, MgO, SiC, AlN, MWCNT, and Cu nanoparticles at a 50/50 vol ratio. The study investigated the effects of volume flow rate, fluid inlet temperature, and Reynolds number for a heat flux of 50 W/cm2. The Al2O3 + MWCNT hybrid nanofluid exhibited a notable increase in convective heat transfer coefficient and a reduction in thermal resistance. Overall, hybrid nanofluids proved to be a superior option for electronics cooling compared to DI water, with Al2O3 + AlN hybrid nanofluid showing promising performance in terms of heat transfer efficiency and coefficient of performance.

In continuation of their earlier research, Vivek Kumar and Jahar Sarkar [19] conducted a subsequent study on the hydrothermal behavior of a hybrid nanofluid containing dissimilar particles in a minichannel heat sink. This hybrid nanofluid comprised varying volume ratios of Al2O3 and MWCNT. The results demonstrated an increase in convective heat transfer coefficient, Nusselt number, pressure drop, and friction factor with a higher MWCNT fraction. The most significant enhancement, at 44.02%, in convective heat transfer coefficient was observed with the MWCNT (5:0) hybrid nanofluid compared to water. The optimal volumetric mixing ratio was found to be approximately 3:2, providing the best heat transfer coefficient to pressure drop ratio. The study concluded that nanofluids exhibit superior performance compared to conventional fluids, and the experimental data facilitated the development of high-quality correlations for Nusselt number and friction factor.

S S Ghadikolaei [20] employed the RKF-5 method to investigate the 3D natural convection Magnetohydrodynamics flow of a GO-MoS_2/Water-Ethylene glycol hybrid nanofluid, examining thermal ray, shape, and slip factors. The results emphasized the

influence of these parameters on velocity profiles and the bonds between fluid molecules. The hybrid nanofluid's robust hydrogen bonding resulted in heightened thermal conductivity and temperature. Moreover, higher shape factors were observed to increase temperature and heat transfer rates while simultaneously reducing hydrogen bonds.

Researchers have also directed their efforts towards improving the cooling of both photovoltaic and electronic systems by exploring the use of nanoparticles and nanofluids.

P C Mukesh Kumar and C M Arun Kumar [21] conducted an investigation into the heat transfer rate, surface temperature, Nusselt number, thermal resistance, power consumption, and reliability of an electronic chip within a six circular channel heat sink. The study involved the use of water and Al_2O_3/water nanofluids as coolants. The ANSYS (v12) Fluent software was utilized to analyze the electronic chip's performance. Results indicate that Al_2O_3/water nanofluids lead to a decrease in surface temperature, power consumption, and thermal resistance compared to water. Additionally, the study found an increase in the Nusselt number, and the reliability of the electronic chip using nanofluids is 70% higher than when water is used as a coolant.

Yuting Jia et al [22] conducted a numerical analysis on a Photovoltaic-Thermal (PV/T) collector utilizing nanofluid. The PV/T collector integrates PV cells and a thermal collector, with nanofluid acting as a coolant to lower the temperature of photovoltaic cells (PV). Mathematical models for the PV/T collector were created to investigate operational parameters. The study explores the impact of nanofluid type and volume concentration on PV conversion efficiency, PV cell temperature, and thermal and electrical power. Results indicate superior performance with Al_2O_3/water nanofluid compared to TiO_2/water nanofluid, and the influence of nanofluid mass flow rate on electrical and thermal power is examined. Varying channel height affects heat removal and thermal power, revealing a 24.00 W difference in thermal power between tube diameters of 0.005 m and 0.015 m.

Amin Taheri et al [23] researched ways to enhance heat transfer in electronic cooling modules. They introduced a novel liquid-based heat sink design by modifying the conventional heat sink heat pipe configuration. Circulating pure water and MWCNT/water nanofluid (0.15% and 0.3%) through the heat sink connected to a printed circuit board, they studied various parameters, including printed circuit board temperature, time to steady-state, average thermal resistance, intermittent load cooling, and energy efficiency. Results demonstrated significant temperature reductions and thermal resistance decreases, with the 0.3% MWCNT/water nanofluid achieving a maximum energy efficiency of 59.2%. Artificial neural networks predicted steady-state board temperatures under different conditions.

Hissouf et al [24] investigated the impact of dispersing Copper (Cu) and Alumina (Al_2O_3) nanoparticles in water on a hybrid Photovoltaic-Thermal (PVT) system. This system provides simultaneous electrical and thermal energy, enhancing overall efficiency. A mathematical model, validated against experimental data, revealed that using Cu-water nanofluid significantly improves performance compared to Al_2O_3-water. With 2% volume fraction of Cu nanoparticles, thermal and electrical efficiencies increased by 4.1% and 1.9%, respectively, over pure water. The model was applied to assess daily power generation in Agadir, Morocco.

In two comprehensive studies, Ghadikolaei investigated the environmental and economic impacts of various cooling methods for photovoltaic (PV) systems. The first study [25] evaluated hybrid approaches, including hybrid microchannel-jet impingement and hybrid phase change materials (PCMs), showing significant improvements in cell efficiency. Combining techniques, like hybrid nano-PCM and hybrid PCM-water, demonstrated even greater advantages in reducing environmental costs associated with CO2 emissions. In a second study [26], Ghadikolaei examined methods to enhance the efficiency and lifespan of solar photovoltaic cells through effective cooling techniques. Emphasizing the critical role of

water flow rate in temperature reduction and cell efficiency, the research highlighted the superiority of jet impingement cooling in hybrid PV-wind systems over conventional PV systems in both cooling rate and energy generation. Phase Change Material (PCM) cooling, particularly in storing heat energy across small temperature differences, proved efficient and adaptable for use with PV cells in various environments.

Nuraini Binti Sukhor et al [27], explored the computational heat transfer characteristics of Al2O3-Cu/water hybrid nanofluid in a micro heat sink. The study involved a working fluid with volume concentrations ranging from 0.1% to 0.5%. Using ANSYS Fluent, they simulated a hexagonal micro-pin fin heat sink with a staggered arrangement, validating results with reliable experimental data. Key findings revealed a consistent increase in Nusselt number with rising Reynolds number, irrespective of concentration and pin spacing. Lower transverse pitch significantly influenced Nusselt number enhancement, resulting in a 10% increase in heat transfer coefficient at 0.5% nanofluid concentration compared to 0.1%. This enhancement was attributed to the transition of Reynolds number into turbulent conditions, especially notable with lower transverse pitch promoting swirling flow. The pressure drop penalty of the working fluid intensified with increased viscous effects of the hybrid nanofluid, particularly at higher concentrations.

Sameh A. Nada et al [28] conducted an extensive experimental study comparing the thermal performance of electronic devices using liquid cooling systems with water, Al2O3, or CuO nanofluids in various mini-channel configurations (serpentine, parallel, and wavy). Findings indicated superior thermal performance in serpentine channels, followed by wavy and parallel configurations. Nanoparticles, particularly CuO, reduced thermal resistance and enhanced the Nusselt number compared to pure water. For serpentine channels at 120 W power density, Nusselt number increased by 4.49%–12.5% with 0.1% vol. Al2O3-water nanofluid and 5.77%–16.01% with 0.1% vol. CuO-water nanofluid. Results were validated against previous analytical/numerical studies and experimental cases.

In another study [29], Ghadikolaei employed 3D Computational Fluid Dynamics (CFD) with the Finite Volume Method (FVM), assessing a green graphene/water nanofluid and two fin designs. Results favored the sinusoidal spiral fin design, with increased sine arcs improving heat transfer and reducing pressure changes. Silver heat sinks outperformed copper and nickel due to higher thermal conductivity. Optimal thermal performance occurred at a nanofluid concentration of φ=0.100%, resulting in a 6.82% improvement, while φ=0.075% yielded a 6.83% enhancement.

In a separate CPU thermal management study [30], Ghadikolaei explored heat transfer in a liquid block using covalently functionalized graphene nanoplatelets (CGNPS/H2O) green nanofluid. Assessing different nature-inspired baseplate designs for CPU cooling, the results favored the spider netted baseplate, reducing the maximum temperature by 8.5K compared to ternate veiny. The heat transfer coefficient varied with nanofluid concentration and Reynolds number, achieving optimal performance with CGNPS 0.1% wt/H2O at Re=2000. The highest thermal enhancement of around 8.5K occurred with the spider netted baseplate design and CGNPS 0.057% wt/H2O nanofluid flow in the liquid block. Both studies integrated nanofluid properties through a User Defined Function (UDF) in ANSYS-Fluent 2021 R2.

The existing literature contains few studies utilizing hybrid nanofluids for electronic device thermal management. Particularly, the effect of different hybrid nanofluid concentration on thermal characterization of micro-heat sinks has received less attention. Similarly, studies specifically dedicated to this field are also scarce, underscoring the need for further exploration in this area.

This study aims to address this gap by conducting a numerical investigation of laminar forced convection flow in a wide rectangular microchannel using nanofluids. The channel is designed with a bottom of finite thickness to hold a heat source or electronic component. We have adopted an innovative approach by using a combination of alumina (Al_2O_3) and silver

(Ag) nanoparticles in ethylene glycol as the base fluid. This particular combination was chosen for its advantageous thermal properties, intending to maximize the efficiency of electronic cooling. The study examines the impact of variables such as Reynolds number, volume concentration of pure nanoparticles, volume concentration of hybrid nanoparticle mixtures, and nanoparticle size on flow and heat transfer characteristics.

2. Numeric model

2. 1. Geometric description

The basis for the current study originates from the experimental work conducted by Mohammad Kalteh et al. [8]. The channel's dimensions are as follows: a length of L= 94.3 mm, a width of w = 28.1 mm, and a height of h_f = 580 µm. The channel has a finite thickness at its bottom (solid region) with a value of h_s= 203 µm, intended for accommodating a heat source or electronic component. Heat is applied uniformly from the bottom at a constant heat flux (q_0=20.5 kW/m^2), while the top surface is considered adiabatic. It is appropriate to regard the flow within the channel as two-dimensional because the channel's width significantly exceeds its height ($w/h_f > 164$), as illustrated in Fig.1.

The considered geometry, akin to a heat sink, is vital in electronic devices. It excels in cooling solutions for high-performance processors or integrated circuits on printed circuit boards. The heat sink's design, with a finite base thickness, efficiently dissipates electronic component heat, ensuring optimal temperatures and preventing overheating issues.

2.2. Governing equations and Thermophysical properties of nanofluid

The study employed the 2-D Navier–Stokes and energy equations to model microchannel flow and heat transfer. The assumptions made are:

(i) the nanofluid behaves as a Newtonian and incompressible fluid,
(ii) laminar flow conditions exist.
(iii) constant thermophysical properties are attributed to the nanofluid.
(iv) Spherical nanoparticles are assumed. and a single-phase model is applied.
(v) The influence of gravity and other body forces is negligible.

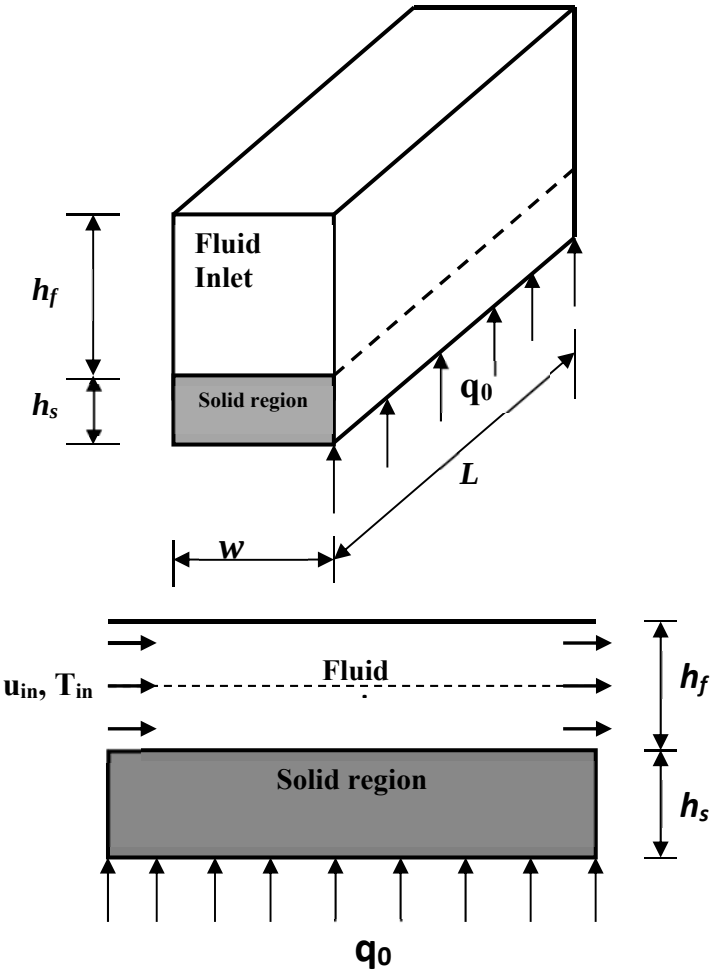

Fig. 1. Diagram illustrating the computational

Laminar flow is considered a suitable option for electronic cooling in this context for various reasons:

Predictability and Control: Laminar flow is more predictable and easier to control than turbulent flow. In electronic cooling applications, precise control of the coolant flow around sensitive electronic components is crucial to maintain uniform temperatures.

Heat Transfer Efficiency: In certain situations, especially when dealing with microscale features or intricate electronic components, laminar flow can provide efficient heat transfer. It ensures that the coolant makes consistent contact with the surfaces to facilitate effective heat dissipation.

Reduced Pressure Drop: Laminar flow typically results in lower pressure drop compared to turbulent flow. This means that the cooling system can operate with lower pumping power, reducing energy consumption.

Less Noise and Vibration: Turbulent flow can generate more noise and vibration compared to laminar flow. In sensitive electronic environments, minimizing noise and vibration can be important.

Avoidance of Hot Spots: In electronic packages, it's crucial to avoid hot spots that can lead to overheating and component failure. Laminar flow can help distribute the coolant more evenly, reducing the likelihood of hot spots.

In Cartesian coordinates, the equations that govern the flow are as follows:

Continuity equation:

$$\frac{\partial u}{\partial x}+\frac{\partial v}{\partial y}=0 \qquad \textbf{(1)}$$

Momentum equation:

$$u\frac{\partial u}{\partial x}+v\frac{\partial u}{\partial y}=-\frac{1}{\rho_{nf}}\frac{\partial p}{\partial x}+\mu_{nf}\left(\frac{\partial^2 u}{\partial x^2}+\frac{\partial^2 u}{\partial y^2}\right) \qquad \textbf{(2)}$$

$$u\frac{\partial v}{\partial x}+v\frac{\partial v}{\partial y}=-\frac{1}{\rho_{nf}}\frac{\partial p}{\partial x}+\mu_{nf}\left(\frac{\partial^2 v}{\partial x^2}+\frac{\partial^2 v}{\partial y^2}\right) \qquad \textbf{(3)}$$

Energy equation:

$$u\frac{\partial T}{\partial x}+v\frac{\partial T}{\partial y}=\frac{K_{nf}}{\rho_{nf}C_{Pnf}}\left(\frac{\partial^2 T}{\partial x^2}+\frac{\partial^2 T}{\partial y^2}\right) \qquad \textbf{(4)}$$

The velocity components in the x-direction and y-direction are represented by 'u' and 'v,' respectively, while 'T' denotes the temperature of the fluid. The effective properties of nanofluids, including density (ρ), specific heat (Cp), dynamic viscosity (μ), and thermal conductivity (k), can be determined using the equations proposed by Pak and Cho [31] and Xuan and Roetzel [32]

$$\rho_{nf}=(1-\phi)\rho_{bf}+\rho_{np}\phi_{np} \qquad \textbf{(5)}$$

$$(\rho C_P)_{nf}=(1-\phi)(\rho C_P)_{bf}+\phi(\rho C_P)_{np} \qquad \textbf{(6)}$$

In this paper, the model developed by Patel et al. [33] is employed to calculate thermal conductivity. This model takes into account factors such as nanoparticle Brownian motion, nanoparticle diameter, volume concentration of nanoparticles (ϕ), and the nanofluid temperature (T) to estimate the thermal conductivity. Here, (ρCp) represents the heat capacity of the fluid, with subscripts "p" denoting nanoparticles, "b_f" indicating the base fluid, and "n_f" representing the effective properties of the nanofluid.

$$\frac{K_{nf}-K_{bf}}{K_{bf}}=\frac{K_{np}}{K_{bf}}\left[1+c\frac{u_P d_{np}}{\alpha_{bf}}\right]\frac{d_{bf}}{d_{np}}\frac{\phi}{1-\phi} \qquad \textbf{(7)}$$

The constant 'c' is set at a fixed value of 25,000 based on a wide range of experimental data, as reported in [33]. The Brownian velocity for nanoparticles, denoted as 'up,' can be calculated using the following method:

$$u_P=\frac{2k_B T}{\pi\mu_{bf}d_P^2} \qquad \textbf{(8)}$$

The formula for calculating the Brownian velocity of nanoparticles, denoted as 'u_p,' incorporates several key parameters: the Boltzmann constant (k_B = 1.038E-23 J/K), particle diameter (d_{np}), molecular size of the liquid (typically 3 Å for water, represented as d_{bf}), volume fraction of particles in the liquid (ϕ), nanofluid temperature (T), and thermal diffusivity (α_{nf}).

The dynamic viscosity of the nanofluid is determined using the Brinkman equation, as outlined in reference [34].

$$\mu_{nf}=\frac{\mu_{bf}}{(1-\phi)^{2.5}} \qquad \textbf{(9)}$$

The evaluation of the thermophysical properties of nanofluids is crucial for their practical applications, but there is currently no consensus within the research community on the most effective method to describe them. Despite a substantial amount of recent research data, traditional models continue to be favored due to their well-established foundation and ease of application. These models provide a practical framework for understanding and applying nanofluid properties in various real-world scenarios, offering a sufficiently accurate approximation for common applications. Their

successful use in previous studies, where results closely aligned with available experimental data, further justifies their continued use in this field.

Table 1 provides the thermophysical properties of Ethylene glycol and alumina Al2O3 and silver Ag nanoparticles. Meanwhile, **Table 2** presents data on the thermophysical properties of nanofluids containing 40 nm nanoparticles with a volume fraction of 4%. These properties are tabulated for various types of nanoparticles.

Table1 Thermophysical properties for Ethylene glycol and various types of nanoparticles at T=300 K.

Property	Ethylene glycol (EG)	Al_2O_3	Ag
ρ (kg/m3)	998.2	3970	10500
μ (Nm/s)	1.01E-3	-	-
K (W/m K)	0.6028	40	429
C_P(kJ/kg K)	4182.2	765	235

The calculation of Reynolds number, Nusselt number, and friction factor is performed as follows [35]:

$$\mathrm{Re} = \frac{\rho_{nf} u_{av} D_h}{\mu_{nf}} \quad \textbf{(10)}$$

$$Nu = \frac{hD_h}{K_{nf}} = \frac{q_0 D_h}{(T_w - T)K_{nf}} \quad \textbf{(11)}$$

$$f = \frac{24}{\mathrm{Re}} \quad \textbf{(12)}$$

The terms u_m, D_h , h and q_0 represent the following quantities: u_m is the average velocity, D_h is the microchannel hydraulic diameter (calculated as $D_h = 2h_f$), h is the convective heat transfer coefficient, and q0 is the heat transfer flux.

Table 2 Thermophysical properties of nanofluids at 4% volume fractions.

Property	2%Al_2O_3+2%Ag	3.2%Al_2O_3+0.8%Ag	0.8%Al_2O_3+3.2%Ag	Al_2O_3
ρ_{nf} (kg/m3)	1046.616	1168.256	1324.976	1116.016
μ_{nf} (Nm/s)	0.9468E-3	0.9468E-3	0.9468E-3	0.9468E-3
K_{nf} (W/m K)	1.80797	1.2133	2.4028	0.7301
C_{Pnf} (kJ/kg K)	3927.225	3524.17	3097	3693.214

2.3. Mesh and Boundary conditions:

In this study, an unstructured mesh composed of quadrilateral elements were employed. It was refined near the wall to effectively capture the significant high velocity and temperature gradients present in that particular region. The prescribed boundary conditions are outlined as follows:

- Varied velocities corresponding to Reynolds numbers were applied at the microchannel inlet, while the inlet temperature was set at T_{in} =300 K.
- A no-slip boundary condition was enforced along the microchannel walls.
- At the channel's outlet, we apply fully developed flow conditions for both velocity and temperature.
- The upper wall of the channel is treated as an insulator, and an adiabatic boundary condition is applied to it.
- The Three sides of the solid region are subjected to a consistent heat flux, with a value of q_0 =20.5 kW/m^2.
- At the boundary between the solid and fluid regions, the heat fluxes and temperatures are equal.

2.4. Numeric Parameters and Processes:

The Fluent software was utilized to address the current problem, enabling the resolution of a set of nonlinear differential equations. Fluent employs the finite volume method to transform the governing equations into a set of algebraic equations that can be solved numerically. The resulting algebraic discretized equations, obtained through spatial integration, are

sequentially solved across the entire considered physical domain. To handle convective and diffusive terms, a second-order upwind method was applied. The coupling of pressure and velocity was achieved using the Semi-Implicit Method for Pressure-Linked Equations Consistent (SIMPLEC). SIMPLEC can often strike a favorable balance between precision and computational efficiency. In microscale simulations, where a high level of detail is necessary to capture small-scale phenomena, computational efficiency becomes paramount. Additionally, the issue of convergence may further underscore the importance of employing an algorithm like SIMPLEC, which is known for its robust convergence properties.

Throughout the simulation, the residuals resulting from the integration of governing equations **(1)**, **(2)**, **(3)**, and **(4)** served as convergence indicators over finite control volumes. These residuals were continuously monitored and scrutinized during the process, ensuring a converged solution was maintained, with residual levels reaching as low as approximately 10^{-8}.

2.5. Grid testing and code validation

A grid independence test was conducted using pure ethylene glycol (EG) at a Reynolds number (Re) of 1500. Three different grid sizes were employed for simulating heat transfer in a microchannel, specifically grid sizes of 40×300, 50×300, and 55×300. The Nusselt number, which characterizes heat transfer, showed minimal variation among these grid sizes. As a result, the 50×300 grid size was selected to reduce computational time. To validate the accuracy of the numerical model, comparisons were made with experimental and existing numerical data from the literature. Validation was performed at Reynolds number Re = 100, using a standard test case of fully developed forced convection flow between parallel plates. In this setup, the top plate is insulated, and the bottom plate maintains a uniform heat flux. The literature reports a Nusselt number of **5.385** and a friction factor of **24** for this flow case [35]. The present study yielded results that closely matched these values, as illustrated in Figure 2.

The accuracy of the results was further confirmed through validation using Al_2O_3 nanofluid. The average Nusselt number values were compared for two different concentrations, namely 0.1% and 0.2% alumina-water nanofluid, across various Reynolds numbers. The comparisons were made against experimental data from reference [8], and the findings are summarized in **Table 3**.

For the 0.1% nanofluid concentration, the present numerical results aligned well with the experimental data, exhibiting a maximum deviation of less than 6%. However, for the 0.2% nanofluid concentration, there were deviations from the experimental results. These deviations could be attributed to a couple of factors: **(i)** The dispersion of nanoparticles within the base fluid may not have been entirely homogeneous, even though it was assumed to be a homogeneous mixture in the numerical model. **(ii)** The correlations used for estimating the effective thermophysical properties of the nanofluid at low volume concentrations might be less accurate, leading to discrepancies between the numerical and experimental results. Nevertheless, it's noteworthy that the present numerical results closely matched the numerical findings reported by Mohammad Kalteh et al for Reynolds number $200 \leq Re \leq 1000$, concentration volume $0\% \leq \varphi \leq 4\%$, and 40 nm nanoparticle size, fig.3.

Table 3 Comparison of the average Nusselt number values with experimental data. **[8].**

Nanofluid	Reynolds number, Re	Nu (experimental)	Nu (present)
0.1%Al_2O_3 +water	225	7.4	6.95
	286	7.7	7.4
0.2%Al_2O_3 +water	204	7.5	6.7
	243	8.1	7.0

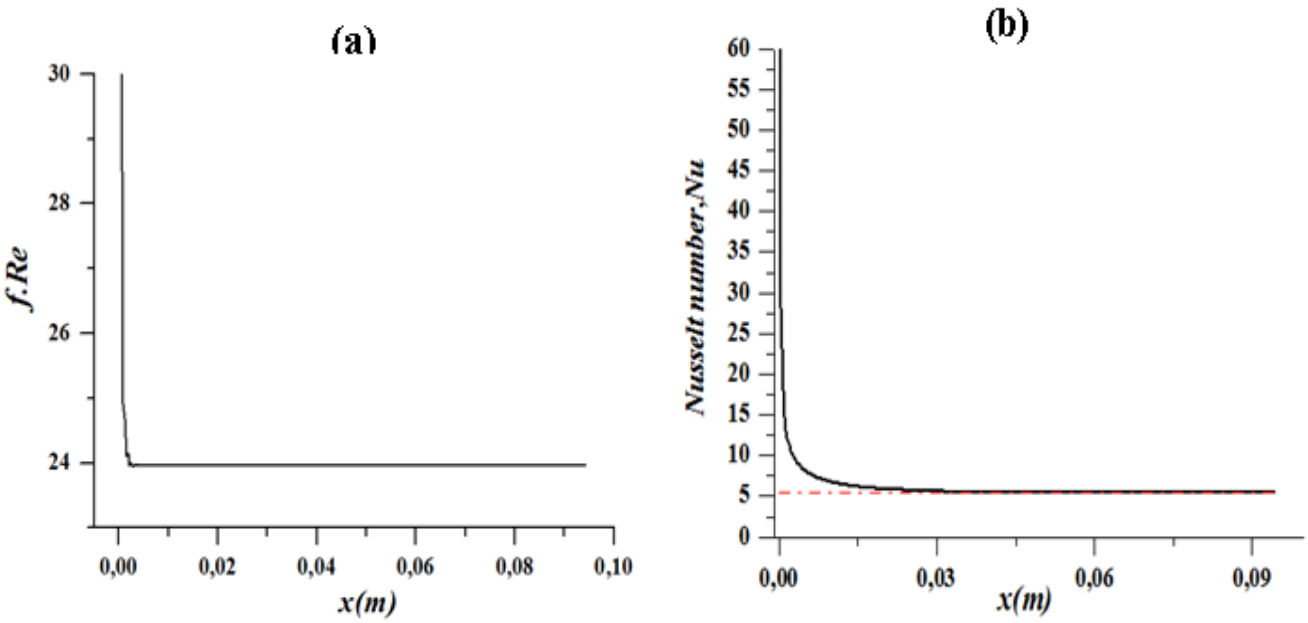

Fig.2 Local friction factor **(a)** and Nusselt number **(b)** for Re=100.

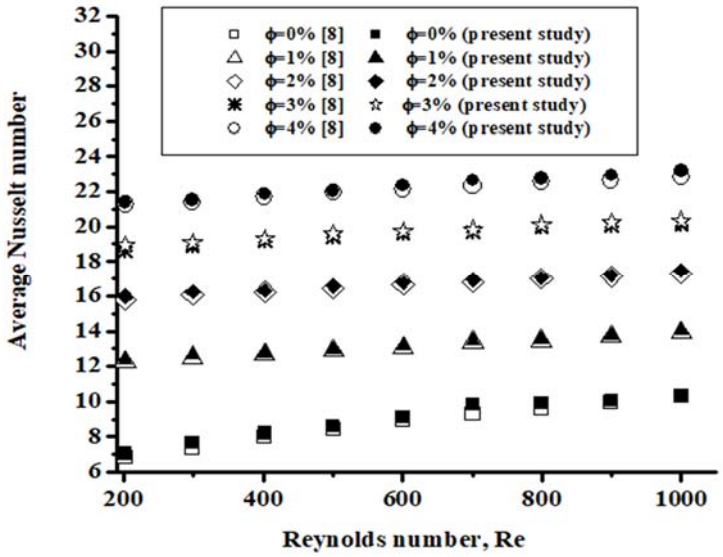

Fig.3 Average Nusselt number for nanofluid in different Reynolds and volume concentrations for 40 nm nanoparticle size.

3. Results and discussion

Simulations were conducted using ethylene glycol as the base fluid with Al2O3 and hybrid (Al2O3+ Ag) nanofluids. The Reynolds number values ranged from 50 to 1500, while four different volume fractions of nanoparticles were considered within the range of 0 to 4. The nanoparticles had diameters varying from 40 nm to 100 nm.

The chosen parametric values, such as increasing volumetric concentration from 0 to 4% and Reynolds number from 100 to 1500, are justified by the potential for internal heat generation due to viscous forces, leading to a temperature rise even in the presence of adiabatic walls. This thermal variation, resulting from viscous dissipation, brings about substantial adjustments in the thermo-physical properties of the fluid between the inlet and outlet of the microchannel.

These changes notably manifest as a reduction in both the friction coefficient and Nusselt number.

These parameter choices were deliberately made to uncover and understand any unexpected flow behavior. This is crucial for obtaining robust and comprehensive conclusions from this study.

The choice of a specific nanoparticle size range, such as 40 to 100 nm, is influenced by several factors:

Thermal Efficiency: Nanoparticles in this size range strike a balance between specific surface area (which affects thermal efficiency) and suspension stability in the fluid. They are small enough to enhance the thermal conductivity of the nanofluid, yet large enough to avoid excessive agglomeration.

Suspension Behavior: Nanoparticles ranging from 40 to 100 nm tend to remain well dispersed in the fluid. This is crucial for maintaining the properties of the nanofluid stably over an extended period.

Avoiding Quantum Size Effects: At much smaller sizes (less than 10 nm), nanoparticles can begin to exhibit quantum properties that may complicate their thermal behavior. By staying within the range of 40 to 100 nm, undesirable quantum effects are avoided.

3.1. The effect of nanofluids:

In this section, we aimed to explore the impact of different types of nanoparticles on thermal and flow characteristics at a Reynolds number (Re) of 600. Specifically, we evaluated the performance of alumina (Al_2O_3) and hybrid (Al_2O_3+ Ag) nanofluids, both with a volume fraction of 4% and particle diameter of 40 nm. The nanofluid that exhibited the most desirable results would be selected as the superior choice.

As depicted in Fig. 4(a), it can be noted that the velocity of the hybrid nanofluid containing 0.8% Al_2O_3 and 3.2% Ag is lower in comparison to pure ethylene glycol and other working fluids. This phenomenon is primarily attributed to the fact that the (0.8% Al_2O_3+3.2% Ag) nanofluid possesses a lower kinematic viscosity ($\nu_{nf} = \mu_{nf} / \rho_{nf}$), as indicated in Table 2. This particular property hinders the rapid movement of (0.8% Al_2O_3+3.2% Ag) particles within the microchannel.

Looking at Fig.4(b) and examining the friction factor, it becomes evident that altering the type of nanofluid does not have any noticeable impact on the trend of the friction factor. Across all the nanofluids tested, they exhibit a consistent trend and maintain the same friction factor value. Furthermore, this figure also demonstrates that the obtained friction factor results closely align with the theoretical prediction value of (f.Re = 24), validating the agreement between the experimental and theoretical outcomes.

Figs. 5(a) and (b) present the average convective heat transfer coefficients and wall temperature, respectively.

In Fig. 5(a), the average convective heat transfer coefficients and wall temperature are displayed. It is evident that, for all the tested nanofluids, there is a noticeable increase in convective heat transfer coefficient within a short distance from the microchannel inlet. However, this coefficient decreases rapidly as the axial coordinate progresses. Throughout the remainder of the microchannel length, the convective heat transfer coefficient remains relatively stable. Notably, the (0.8% Al_2O_3+3.2% Ag) nanofluid stands out with the highest convective heat

transfer coefficient when compared to pure EG and other working fluids. This can be attributed to its superior thermal conductivity, as indicated in **Table 2**.

Fig.5(b) reveals that the hybrid (0.8% Al_2O_3+3.2% Ag) nanofluid achieves a lower wall temperature than pure EG and pure oxide (Al_2O_3) nanofluid. This improvement is attributed to the significantly higher thermal conductivity of (0.8%Al_2O_3+3.2%Ag) compared to EG, resulting in a more efficient energy exchange and enhanced heat transfer between the fluid and the microchannel wall.

(a)

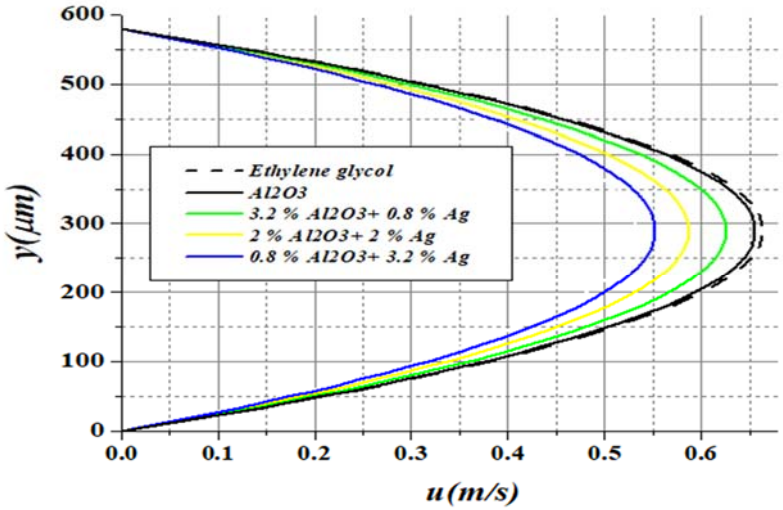

(b)

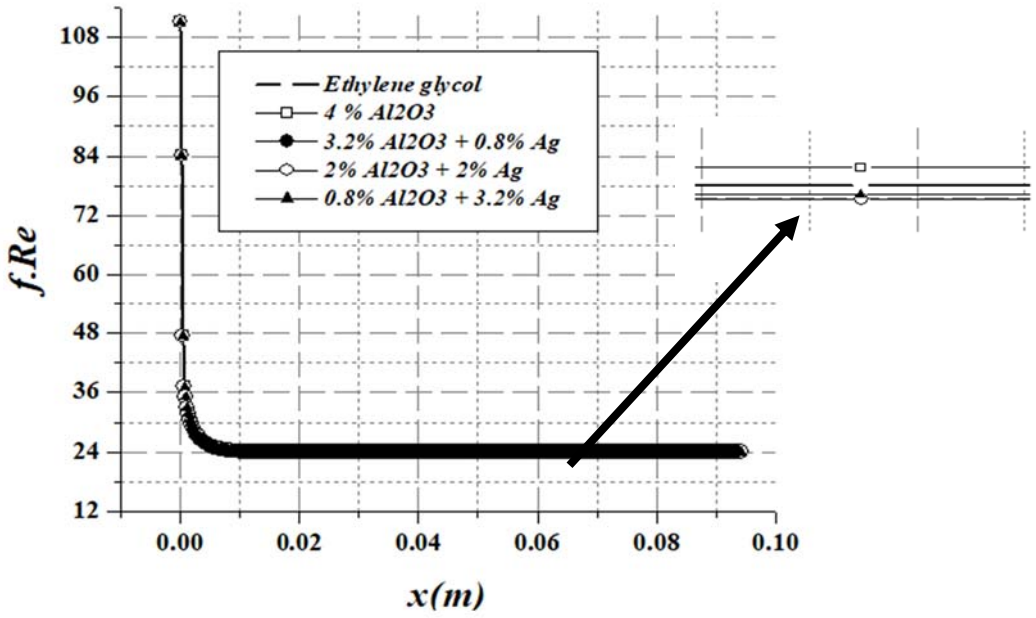

Fig. 4. Velocity profile (**a**) and friction factor **(b)** as functions of position for various nanofluids, Re=600.

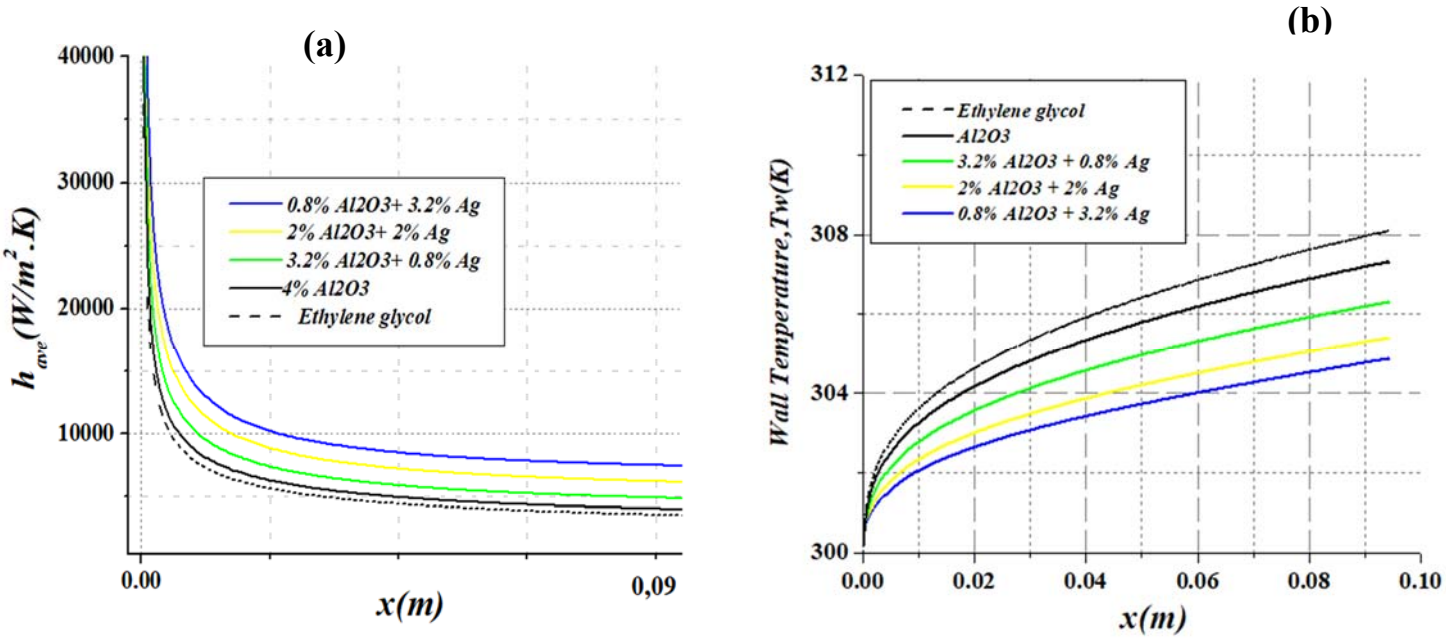

Fig.5. Evolution of the local convective heat transfer coefficient **(a)** and wall temperature **(b)** along the channel length for various nanofluids at Re = 600.

The graph in Fig.6 illustrates the average convective heat transfer coefficients for ethylene glycol and various nanofluids at different Reynolds numbers. It's evident that the average convective heat transfer coefficient for a specific nanofluid increases as the Reynolds number increases, primarily due to the higher inlet fluid velocity. Furthermore, it's worth noting that the hybrid nanofluid exhibits the highest average convective heat transfer coefficient when compared to alumina (Al_2O_3) nanofluid and pure ethylene glycol. In laminar flow, the heat transfer coefficient is primarily influenced by the fluid's thermal conductivity. However, at higher flow rates, factors such as the dispersion effects and chaotic movement of nanoparticles enhance mixing fluctuations and lead to a flatter temperature profile, resembling turbulent flow. This effect results in an increase in the heat transfer coefficient. For instance, at Re = 1500, the average convective heat transfer coefficient of the hybrid nanofluid (0.8% Al_2O_3 + 3.2% Ag) is enhanced by 83% compared to pure EG.

In summary, these results highlight the superior efficiency of the (0.8% Al2O3 + 3.2% Ag) hybrid nanofluid. While the production cost of pure oxide (Al_2O_3) nanofluid remains high (approximately $535 for 25g), hybrid nanofluids enhance heat transfer characteristics while reducing the cost of the working fluid due to a lower volume fraction of pure oxide nanoparticles. Depending on the cooling requirements, suitable proportions of mixed nanoparticle volume concentrations can be selected.

3.2. The effect of different nanoparticles volume fractions:

To study the influence of nanoparticles volume fractions on thermal and flow fields, the range of the nanoparticle volume fraction is varied from 0% to 4%. The 0% concentration is related to pure EG with no nanoparticle. Al2O3-Ag hybrid nanofluid is chosen as working fluid. The diameter of particle dp=40 nm and the Reynolds number is fixed at Re=600.

In Fig.7(b), it's evident that, for the considered axial position, there is a substantial reduction of nearly 4 K in wall temperature when comparing the case with a particle volume fraction (φ) of 4% to the case without particles (φ = 0%). What's noteworthy is that this reduction

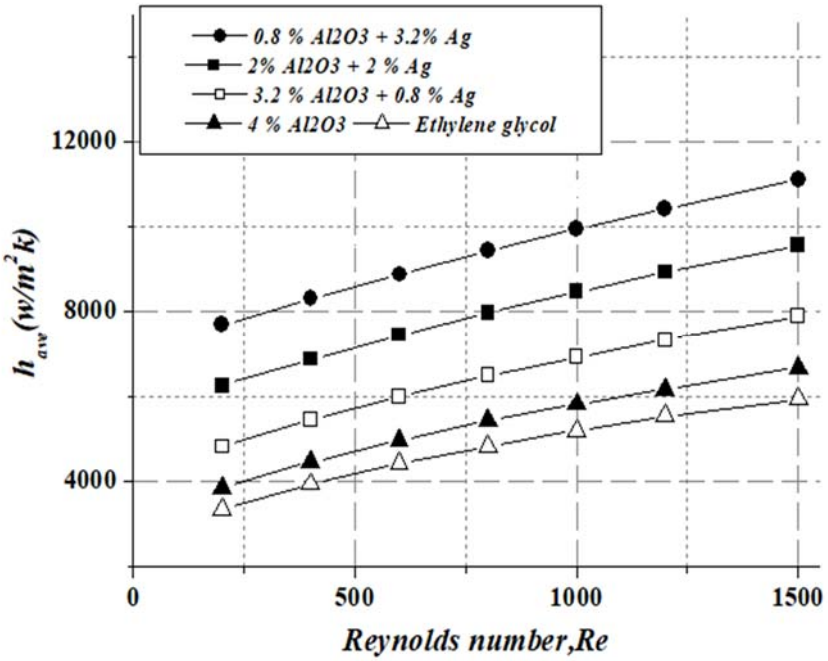

Fig.6. Average convective heat transfer coefficient for different nanofluids and for Reynolds numbers.

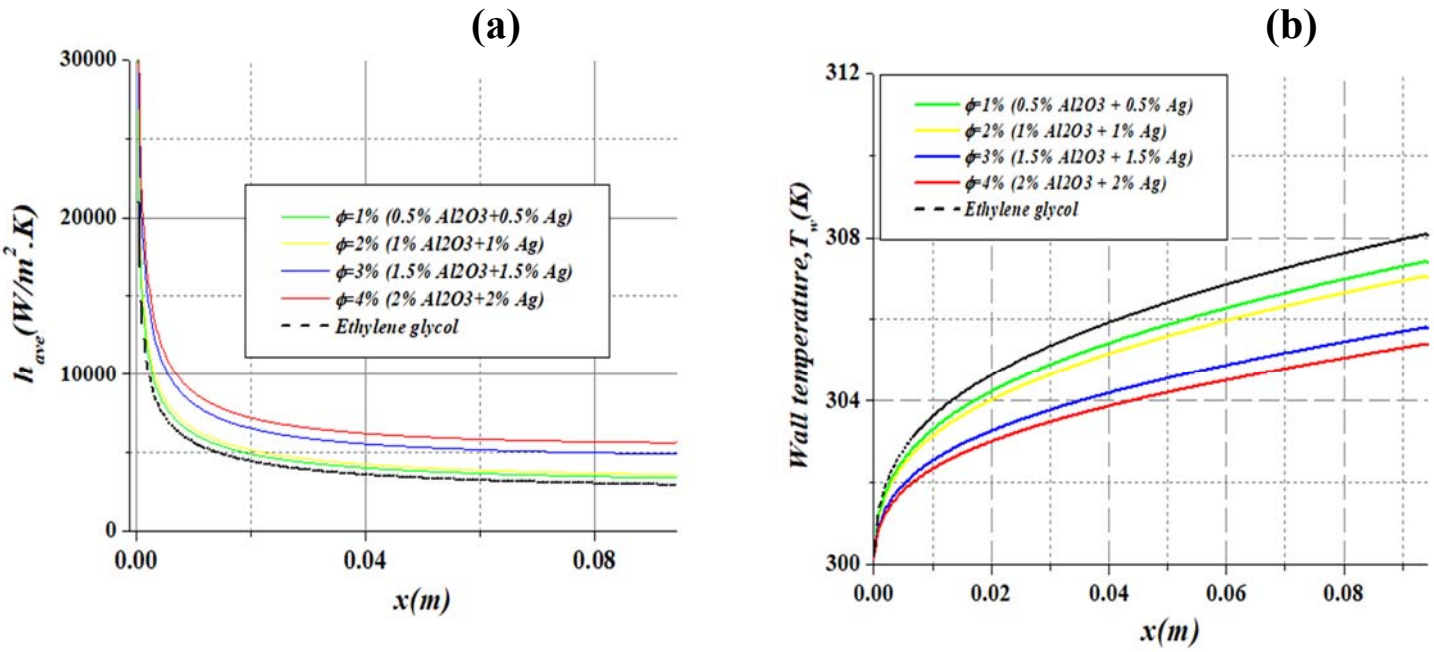

Fig 7. The effect of different nanoparticle concentrations versus position on: **(a)** heat transfer coefficient, **(b)** Temperature wall. Re=600.

in fluid temperature at the microchannel wall persists along the entire length of the microchannel and appears to be more pronounced towards the exit. These results clearly demonstrate the beneficial effects of nanoparticles, effects that can be attributed to the fact that the presence of such particles significantly enhances the thermal properties of the resulting mixture. For instance, at a specific φ value of 4%, it was observed that the thermal conductivity (k) values increased by up to 200% compared to those corresponding to the case with φ = 0% (as shown in Table 2). The nanofluid inherently offers higher thermal conductivity than the base (conventional) fluid. Additionally, the higher thermal conductivity of the mixture leads to more effective wall-to-fluid heat transfer, as reflected in the subsequent results.

Fig.7(a) highlights that the utilization of nanofluid indeed results in a significant enhancement of heat transfer at the microchannel wall. For instance, at the specific φ value of 4%, the convective heat transfer coefficient reaches approximately 5700 W/m²·K near the end of the microchannel. This indicates a substantial increase of 90% in the heat transfer coefficient compared to that of the base fluid. The augmentation in the volume fraction of nanoparticles intensifies the interaction and collision of these particles. Moreover, the diffusion and relative movement of these particles near the channel walls promote rapid heat transfer from the walls to the nanofluid.

In Fig. 8(a), it is evident that a 4% concentration leads to the lowest velocity compared to other concentrations. This is primarily due to the increase in fluid viscosity with the rise in concentration, which hampers the movement of particles within the microchannel.

Notably, there was no noticeable change in the friction factor for various concentration values, as depicted in Fig. 8(b). The friction factor of the tested nanofluids closely aligns with the friction factor value for pure EG, highlighting one of the significant advantages of hybrid nanofluids.

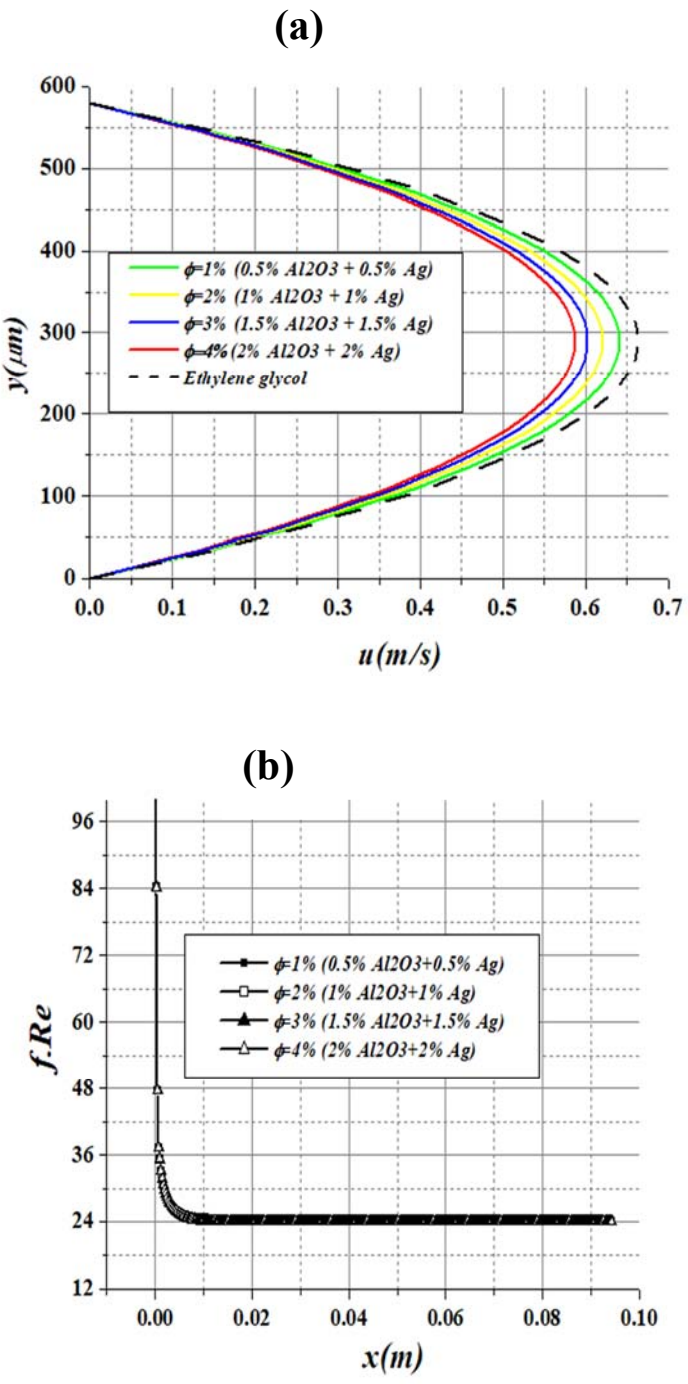

Fig. 8. Velocity profile (**a**) and friction factor **(b)** versus position for different types of nanofluids, Re=600.

3.3. The effect of Reynolds number:

To explore the impact of different Reynolds numbers on thermal and flow characteristics, we considered a nanofluid with a volume fraction of 4% (2% Al_2O_3 - 2% Ag) and particle diameter of 40 nm. The Reynolds number range investigated spanned from 50 to 1500.

As depicted in Fig 9(a), the highest Nusselt number was observed at the highest Reynolds number of 1500. Similarly, in Fig 9(c), the highest Reynolds number yielded the highest velocity compared to lower Reynolds numbers. An increase in Reynolds number resulted in a subsequent increase in velocity. This higher velocity facilitated rapid particle movement and collision, subsequently enhancing the heat transfer rate and reducing wall temperature, as illustrated in Fig. 9(b).

Additionally, the highest-pressure drop increased with increasing Reynolds numbers, as shown in Fig.9(d). The effects of Reynolds number on the local friction factor are evident in Fig. 9(e). It's worth noting that each case began with a relatively high friction factor but eventually converged towards an approximate value consistent with fully developed flow theory (f.Re=24) as the flow reached the exit of the microchannel.

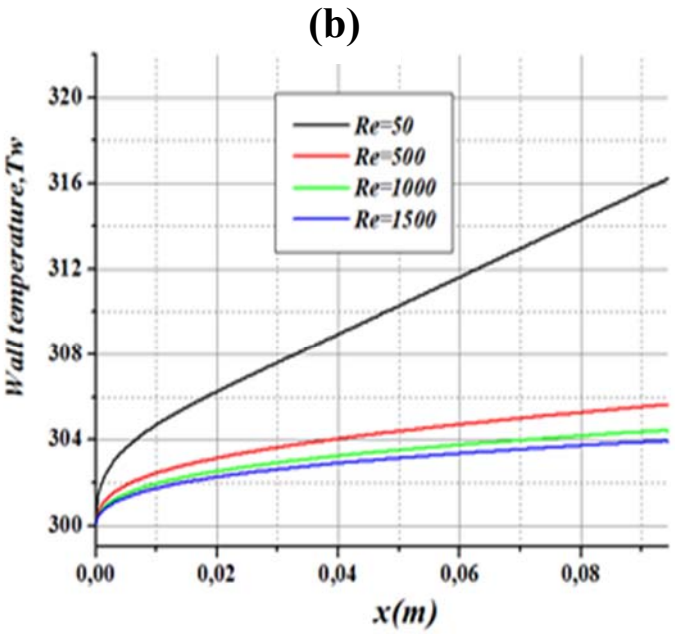

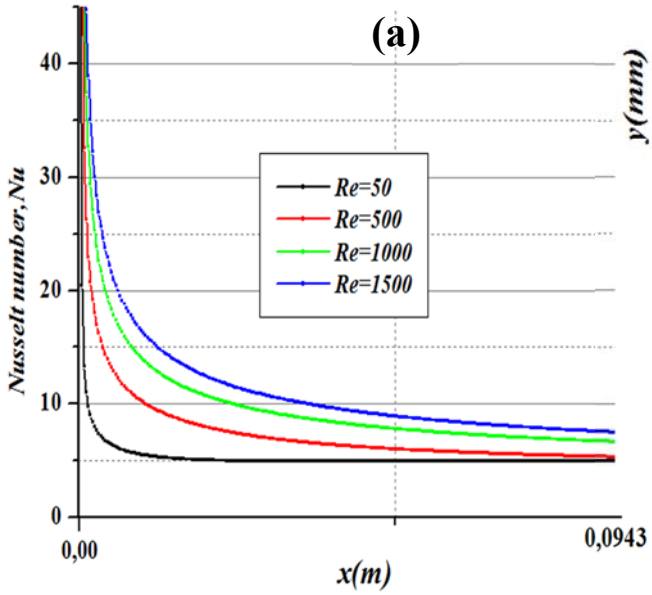

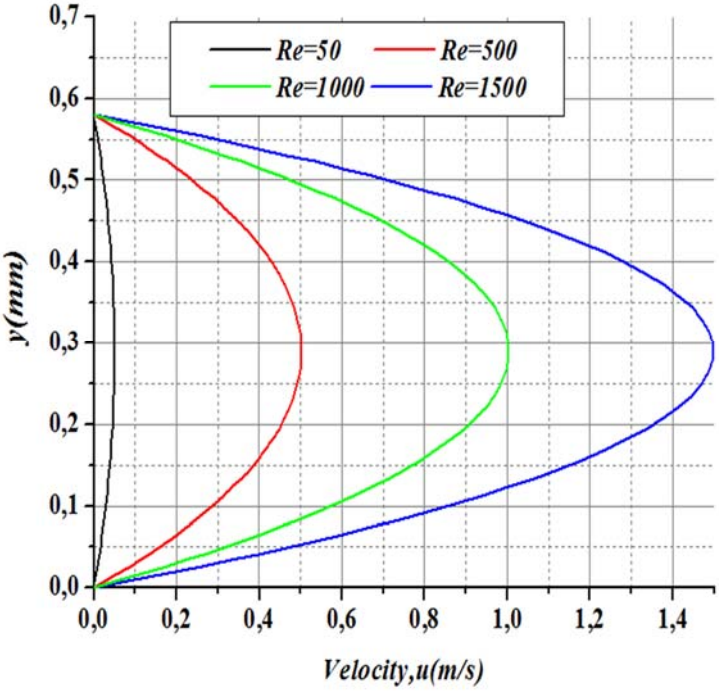

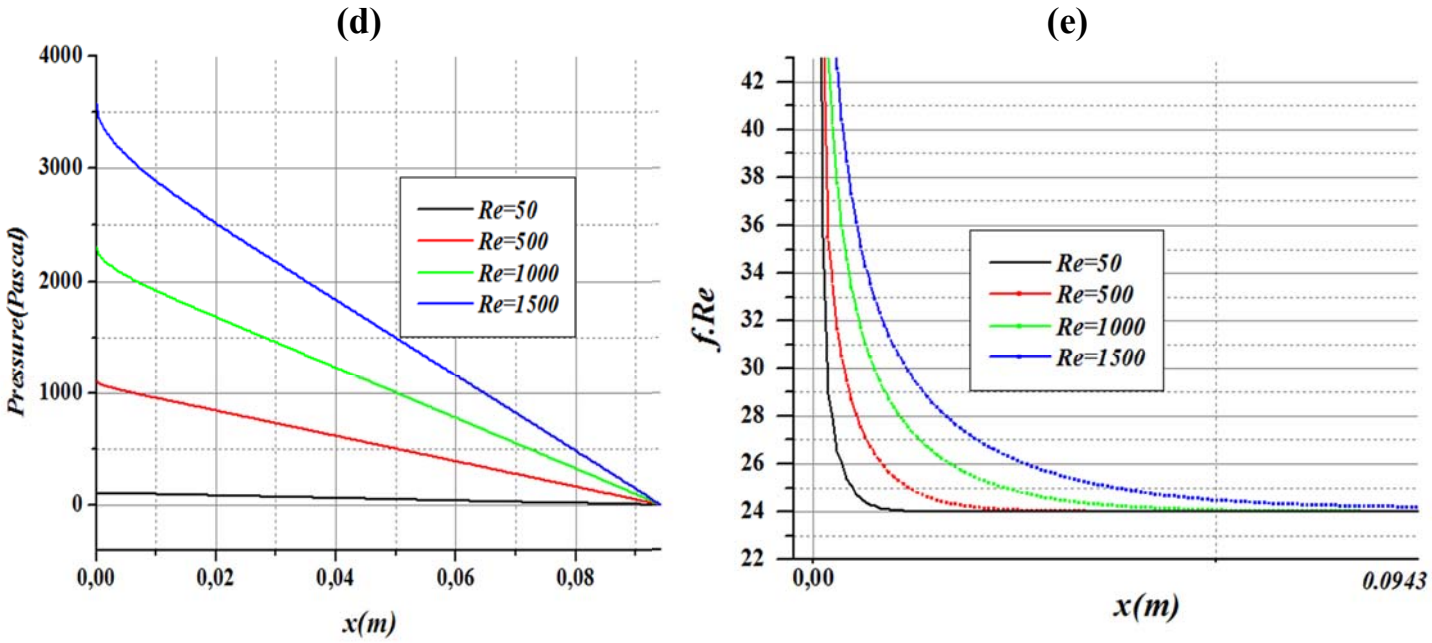

Fig. 9. The effect of different Reynolds numbers versus position on: **(a)** Nusselt number, **(b)** wall temperature **(c)** Velocity profile **(d)** pressure drop and **(e)** friction factor.

3.4. The effect of nanoparticle diameter

Fig 10(a) illustrates the average convective heat transfer coefficient for 4% (2% Al_2O_3 - 2% Ag) nanofluids with varying nanoparticle sizes and volume fractions at Re = 500. It's evident from Fig 10(a) that the convective heat transfer coefficient increases as the nanoparticle diameter decreases, especially at higher concentrations. For instance, at $\varphi = 4\%$, reducing the diameter of Al_2O_3-Ag nanoparticles from 100 nm to 40 nm results in a 58% increase in the convective heat transfer coefficient. This increase in heat transfer is primarily attributed to the higher surface area-to-volume ratio of smaller nanoparticles, allowing for more efficient heat absorption and transfer at the particle-fluid interface. Moreover, smaller nanoparticles exhibit a more uniform distribution, whereas larger nanoparticles lead to non-uniform distribution and higher concentrations near the wall, where viscous forces become significant, thus reducing heat transfer enhancement.

Fig 10(b) reveals that fluid temperature decreases with decreasing nanoparticle size, primarily due to the increased effective thermal conductivity of the nanofluid.

In Fig 10(c), fluid velocity remains consistent for different nanoparticle sizes. This constancy is because the velocity field depends on the density nd dynamic viscosity of the flowing fluid, which are not significantly influenced by nanoparticle size variations.

Regarding the friction factor, Fig 10(d) shows no notable change in the friction factor across different nanoparticle sizes. The friction factor results were compared with conventional theory, and it was found that the friction factor results closely match the predictions of conventional theory.

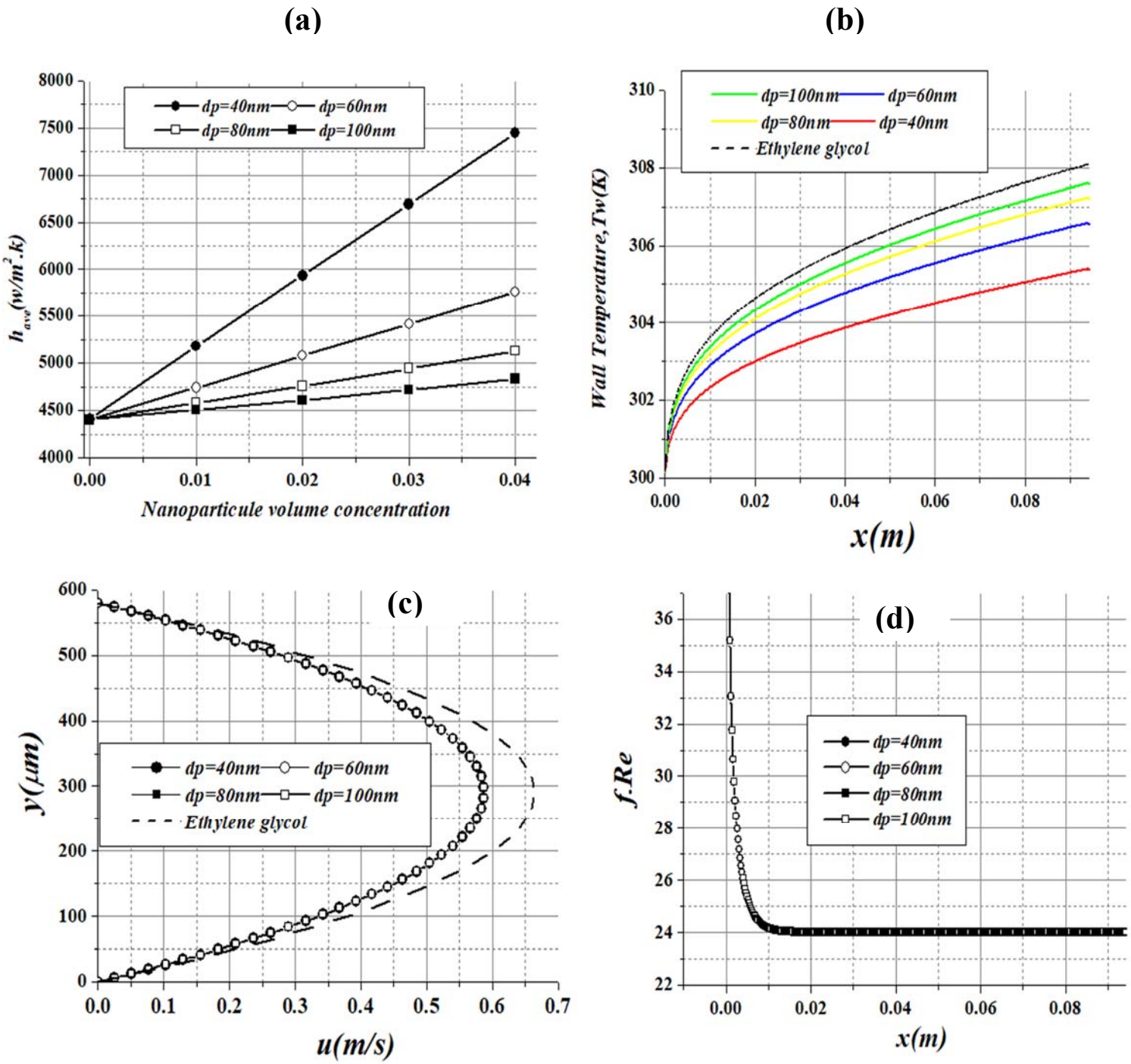

Fig. 10. Effect of the nanoparticle size of the nanofluid on: **(a)** Average convective heat transfer coefficient, **(b)** wall temperature, **(c)** Velocity profile, **(d)** Friction factor.

4. Conclusions

A two-dimensional numerical simulation investigated laminar forced convection heat transfer in a microchannel, focusing on flow field and heat transfer enhancements due to various parameters, including nanofluid types, nanoparticle concentration, nanoparticle diameter, and Reynolds number. The governing equations were solved using the Finite Volume Method with the SIMPLEC algorithm.

The findings indicate that the combination of Al_2O_3 nanoparticles into Ag/ethylene glycol nanofluids, known as hybrid nanofluids, effectively enhances convective heat transfer. Particularly, employing hybrid nanofluids at high volume concentrations (0.8% Al2O3 + 3.2% Ag) and elevated Reynolds numbers Re = 1500 improves heat transfer by 83% compared to pure EG while reducing the working fluid's cost compared to pure alumina nanofluids. Furthermore, increasing Reynolds numbers leads to higher Nusselt numbers, velocities, pressure drops, and friction factors. The average convective heat transfer coefficient increases by 58% with a decrease in nanoparticle diameter, especially at higher concentrations. while particle concentration and diameter have no significant impact on the friction factor.

These results provide valuable insights into flow and heat transfer characteristics of hybrid nanofluids in microchannels and offer guidance for designing thermal systems, particularly for electronics cooling applications.

References:

[1] S U S Choi, J A Eastman, S U S Choi and J A Eastman, Enhancing thermal conductivity of fluids with nanoparticles. Int Mechanical Engineering Congress and Exposition San Francisco, (1995), 66:99–105.

[2] Lee J, Mudawar I, Assessment of the effectiveness of nanofluids for single phase and two-phase heat transfer in micro-channels. Int Comm in Heat and Mass Transfer, (2007), 50(3–4):452–63.

[3] Chein R, Chuang J, Experimental microchannel heat sink performance studies using nanofluids. Int J of Thermal Science, (2007), 46(1):57–66.

[4] V Bianco, F Chiacchio, O Manca, S Nardini. Numerical investigation of nanofluids forced convection in circular tubes. Applied Thermal Engineering, (2009), 29 (17–18): 3632–3642.

[5] Ho C J, Wei L C, Li. ZW, An experimental investigation of forced convective cooling performance of a microchannel heat sinks with Al2O3/water nanofluid. Applied Thermal Engineering, (2010), 30(2–3):96–103.

[6] A R Sajadi, M H Kazemi, Investigation of turbulent convective heat transfer and pressure drop of TiO2/water nanofluid in circular tube. Int Comm of Heat and Mass Transfer, (2011), 38: 1474–1478.

[7] S Suresh, K P Venkitaraj, P Selvakumar and M Chandrasekhar, Effect of Al2O3-Ag/water hybrid nanofluid in heat transfer. Experimental Thermal and Fluid Science, (2012), 38: 54-60.

[8] Mohammad Kalteh, Abbas Abbassi and Majid Saffar-Avval, Experimental and numerical investigation of nanofluid forced convection inside a wide microchannel heat sink. Applied Thermal Engineering, (2012), 36: 260-268.

[9] Xin Fang, Qing Ding, Li-Wu Fan, Thermal conductivity enhancement of ethylene glycol-based suspensions in the presence of silver nanoparticles of various shapes. J of Heat Transfer, (2013), 136: 034501(1-7).

[10] Shariat M, Mokhtari R, Akbarinia A, Rafee R Sajjadi S M. Impact of nanoparticle mean diameter and the buoyancy force on laminar mixed convection nanofluid flow in an elliptic duct employing two phase mixture model. Int Comm in Heat and Mass Transfer, (2014), (50): 15-24.

[11] Farhad A, Abbassi, Mohsen Nazari, and M Shahmardan, Numerical Study of Heat Transfer and Flow Bifurcation of Al2O3 Nanofluid in Sudden Expansion Microchannel Using Two-Phase Model. Modern mechanical engineering, (2017), 07(2): 57-72.

[12] Omid Ali Akbari, Davood Toghraie, Arash Karimipour, The Effect of velocity and dimension of solid nanoparticles on heat transfer in non-Newtonian nanofluid.

Physica E: Low dimensional Systems and Nanostructures, (2017): S1386-47730653.

[13] Vivek Kumar and Jahar Sarkar, Two-phase numerical simulation of hybrid nanofluid heat transfer in minichannel heat sink and experimental validation, Int Comm Heat Mass Transfer, (2018),91: 239-247.

[14] M. K. Nayak. HHR impact on 3D radiative stretched flow of Cu-H2O nanofluid influenced by variable magnetic field and convective boundary condition Int J of Thermofluid Science and Technology, (2019), 6(2): 19060202.

[15] S S Ghadikolaei and M. Gholinia, Terrific effect of H2 on 3D free convection MHD flow of $C_2H_6O_2$single bond H2O hybrid base fluid to dissolve Cu nanoparticles in a porous space considering the thermal radiation and nanoparticle shapes effects Int J of Hydrogen Energy, (2019), 44 17072-17083.

[16] M. Veera Krishna and Ali J Chamkha, Hall effects on MHD squeezing flow of water based nanofluid between two parallel disks, J of Porous Media, (2019),22(2):209-223.

[17] M. Veera Krishna and Ali J Chamkha, Hall and ion slip effects on Unsteady MHD Convective Rotating flow of Nanofluids, Application in Biomedical Engineering, J of the Egyptian Mathematical Society, (2020), 28:1.

[18] Vivek Kumar and Jahar Sarkar, Experimental hydrothermal characteristics of minichannel heat sink using various types of hybrid nanofluids, Advanced Powder Technology, (2020), 31(2): 621-631.

[19] Vivek Kumar and Jahar Sarkar, Particle ratio optimization of Al2O3-MWCNT hybrid nanofluid in minichannel heat sink for best hydrothermal performance, Applied Thermal Engineering, (2020), 165: 114546.

[20] S S Ghadikolaei and M Gholinia, 3D mixed convection MHD flow of GO-MoS_2 hybrid nanoparticles in H_2O–$(CH_2OH)_2$ hybrid base fluid under the effect of H_2 bond, Int Comm in Heat and Mass Transfer, (2020), 110:104371.

[21] P C Mukesh Kumar a, C M Arun Kumar, performance using Al2O3/water nanofluids in six circular channel heat sink for electronic chip, Materials Today: Proceedings, (2020), 21: 194-201.

[22] Yuting Jia, Fengming Ran, Chuqiao Zhu, Guiyin Fang, Numerical analysis of photovoltaic-thermal collector using nanofluid as a coolant, Solar Energy, (2020), 196: 625-636.

[23] Amin Taheria et al, A new design of liquid-cooled heat sink by altering the heat sink heat pipe application: Experimental approach and prediction via artificial neural network, Energy Conversion and Management, (2020), 206: 111485.

[24] Mohamed Hissouf, M'barek Feddaoui, Monssif Najim, Adil Charef, Numerical study of a covered Photovoltaic-Thermal Collector (PVT) enhancement using nanofluids, Solar Energy, (2020), 199: 115-127.

[25] S S C Ghadikolaei, An enviroeconomic review of the solar PV cells cooling technology effect on the CO2 emission reduction" -Solar Energy, 216 (2021) 468-492.

[26] S S C Ghadikolaei, Solar photovoltaic cells performance improvement by cooling technology: An overall review" - International Journal of Hydrogen Energy, (2021), 46: 10939-10972.

[27] Nuraini Binti Sukhora, Alhassan Salami Tijani a, Jeeventh Kubenthiran a, and Ibrahim Kolawole uritala, Computational modeling of thermal characteristics of hybrid nanofluid in micro-pin fin heat sink for electronic cooling, international Journal of Green Energy,(2021),18(10): 1027-1045.

[28] Sameh A Nada, R M El-Zoheiry, M Elsharnoby, O S Osman, Enhancing the thermal performance of different flow configuration minichannel heat sink using Al2O3 and CuO-water nanofluids for electronic cooling: An experimental assessment, International J of Thermal Sciences, (2022), 181:107767.

[29] SS Ghadikolaei, Gholinia, Cheng-Xian Lin, A CFD modeling of CPU cooling by eco-friendly nanofluid and fin heat sink passive cooling techniques, Advanced Powder Technology, (2022) ,33: 103813.

[30] S S Ghadikolaei, M Gholinia, Masoud Rahimi, A CFD modelling of heat transfer between CGNPs/H2O Eco-friendly nanofluid and the novel nature-based designs heat sink: Hybrid passive techniques for CPU cooling, Thermal Science and Engineering Progress, (2023) 37: 101604.

[31] Bock Choon Pak, Young I. Cho. Hydrodynamic and heat transfer study of dispersed fluids with submicron metallic oxide particles. Experimental Heat Transfer, (1998), 11 (2): 151-170

[32] Yimin Xuan, Wilfried Roetzel, "Conceptions for heat transfer correlation of nanofluids", International Journal of Heat and Mass Transfer, (2000), 43 (19): 3701-3707.

[33] Hrishikesh E Patel, T Sundararajan T. Pradeep, A Dasgupta, N. Dasgupta, Sarit K. Das. A micro-convection model for thermal conductivity of nanofluids. Pramana-Journal of Physics, (2005), 65 (5): 863-869.

[34] H.C. Brinkman, The Viscosity of Concentrated Suspensions and Solutions. J of Chemical Physics, (1952), 20(4): 571.

[35] Adrian Bejan, Allan D. Kraus, Heat Transfer Handbook. New Jersey, John Wiley Sons, Inc. Hoboken, 2003

.